Preliminary Design of Energy Storage System and Bidirectional DC-DC Converter for Aircraft application

Hassan Cheaito, Joris Pallier, Pascal Pommier-Petit, Bruno Allard, Guy Clerc, Ali Sari, Pascal Venet

Preliminary Design of Energy Storage System and Bidirectional DC-DC Converter for Aircraft application

Hassan Cheaito
Univ Lyon, INSA Lyon, Univ Claude Bernard, Ecole Centrale Lyon, CNRS, F-69621
Villeurbanne, France
hassan.cheaito@insa-lyon.fr

Joris Pallier
Power Department Centum Adeneo
Ecully, France
jpallier@centumadeneo.com

Pascal Pommier-Petit
Power Department Centum Adeneo .
Ecully, France
ppommier-petit@centumadeneo.com

Bruno Allard, Guy Clerc
Univ Lyon, INSA Lyon, Univ Claude Bernard, Ecole Centrale Lyon, CNRS, F-69621
Villeurbanne, France
bruno.allard@insa-lyon.fr ; guy.clerc@univ-lyon1.fr

Ali Sari, Pascal Venet
Univ Lyon, Univ Claude Bernard, INSA Lyon, Ecole Centrale Lyon, CNRS, F-69621
Villeurbanne, France
ali.sari@univ-lyon1.fr ; pascal.venet@univ-lyon1.fr

***Abstract*—Green solutions have gained rapid popularity in transportation. The more electric aircraft is one of main challenges. This paper deals with the methodology of designing an electronic module able to move aircraft on-ground and recover taxiing energy. The preliminary design addresses a power density of 30 Wh/kg, 60 Wh/dm^3, 2 kW/kg and 2,5 kW/dm^3. The braking phase is nearly 30 s along with peak current up to 150 A. The energy storage unit is based on lithium-ion batteries whereas an interleaving converter appears a good candidate as an architecture to fit with the aeronautic constraints.**

Keywords—Energy Storage System, Lithium-ion Battery, Bidirectional converter (BDC), Silicon Carbide

I. Introduction

Global air traffic is expected to increase dramatically [1]. Without any doubts, this evolution will have a harmful impact on the environment such as increasing the CO2 and NOx emissions. In order to achieve operating improvements as well as reducing costs and environmental impact, the transition to more electrified aircraft systems is currently being explored [2]. Moving aircrafts on ground is an opportunity for saving emissions. Today, aircraft engines designed for flight phases at high power levels are used as power source to move the aircraft on ground. As a result, using the main engines for on ground operations leads to increased fuel burn as the systems are forced to operate in highly inefficient conditions. Fuel consumption from aircraft taxiing (on-ground operation) is forecast to cost 6,4 billion euros and represents the emission of 18M metric tons of CO2 per year [3].

Electric Taxiing (ET) is estimated to save up to 4% of the total fuel used on a flight, especially for short range flights. In addition, the electric taxiing system also allows aircrafts to push back without support from an external tug. Aircrafts equipped with this system are able to operate more quickly, thereby reducing both gate and tarmac congestion. The supply of the ET powertrain is performed through the available main network (ATA 24) which is converted via the Auto-Transformer Rectifier Unit (ATRU) in order to drive the wheel actuator (WA) (see Fig. 1).

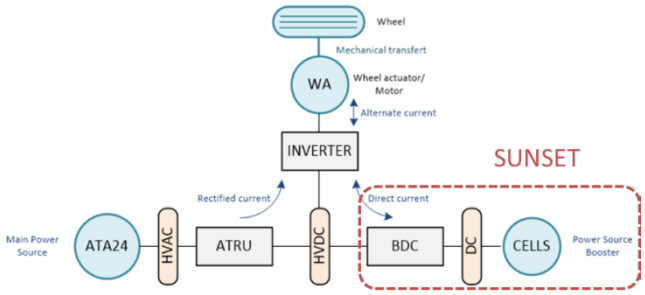

Fig. 1. Synoptic of the functionality of the SUNSET project within the aircraft network.

A project of Storage energy UNit for Smart and Efficient operation on Tarmac (SUNSET) is explored in order to recover energy at braking during the aircraft taxiing phase after landing. This module constitutes a great transition from mechanical brakes to electrical ones, with improved lifetime of the aircraft wheel and brake system.

The paper focuses on the predesign of the SUNSET module. The module has to manage bi-directional energy flow, including conditioning the regenerated power. The overall system should be packaged in a low volume/low mass form factor. This paper discusses the technological trade-off and selection of the technology offering the greatest room for improvement. The design of this module is very challenging because, in addition to the high power and energy densities, it should meet all the aeronautic constraints such as safety, vibration stress, electromagnetic compatibility, thermal management, shock loads, etc. Next section covers a review of solutions for storage to detect a trade-off between power, energy and densities. Section III covers some issues about the power converter that highly depends on the battery technology.

II. Energy Storage System (ESS)

The aim of this project is to design a highly compact power converter storing the energy in regenerative phases with the best class existing technologies. The ideal densities of storage cells to achieve the needed compactness would be around: 30 Wh/kg – 2 kW/kg – 60 Wh/dm^3. Next subsection

describes three main storage technologies: Supercapacitors (SC), Lithium-ion batteries (LIB) and Lithium-ion Capacitors (LIC).

A. Three main ESS

While lead acid cells [4] store and release energy via a redox reaction, LIBs use intercalation; i.e. inserting lithium ions into the electrodes' crystal lattice structure [5]. In the literature, the term "Lithium-ion battery" is widely used when the Li+ ion is elaborated in the cell. Depending on the choice of materials and combinations of the two electrodes, the voltage, the energy density, the lifespan and the safety of a LIB can change dramatically. Fig. 2 shows the main commercialized technologies: Lithium Cobalt Oxide (LCO), Lithium Manganese Oxide (LMO), Lithium Nickel-cobalt-Aluminium oxide (NCA), Lithium Nickel Manganese Cobalt Oxide (NMC), Lithium Iron Phosphate (LFP) and Lithium Titanium Oxide (LTO) [6].

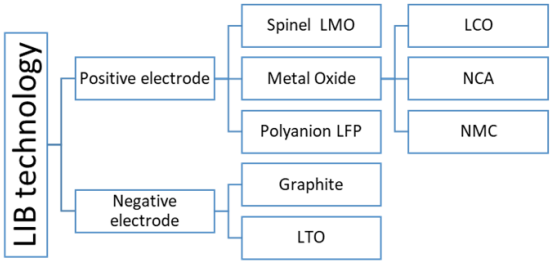

Fig. 2. The different technologies basing on electrodes materials.

In contrary to the behavior of batteries, SCs' storage does not rely on chemical reactions. They do not have any dielectrics either. Also known as Electrical double-layer capacitor (EDLC), the SCs' electrodes are made of active materials such as the activated carbon that adsorb ions present in the electrolyte. The charge is then stored by an electrostatic process rather than a faradaic one. Compared to LIBs, SCs' main advantages are their long lifecycle and high power density. However, their auto-discharge rates are high and their energy densities are low [7].

A new technology that combines both conventional ESSs (SCs and LIBs) is the LIC. The aim of this component is to fill the gap between SCs' low energy density and LIBs' low power density [8]. Several LIC technologies exist. For one of them (for example those of JSR Micro) its positive electrode is similar to the positive electrode of a SC. Similarly, the negative electrode of an LIC is the same as the one of LIBs. So LICs unit may be expressed in Farad or in Ah.

B. Trade-off

Fig. 3 compares the SUNSET targets to the density of the three ESSs according to the suppliers' datasheet. Of course, there are still plenty of products and manufacturers but at least this figure shows a panel which reflects the order of magnitude of the three main ESSs. Fig. 3 confirms the state of art of the main ESS. The SC technology can deliver high power (~10 kW/kg) but only for short time which implies low energy (~7 Wh/dm^3). The LIC can store more energy (~30 Wh/dm^3) but not enough yet to reach our target. However, the LIB easily reaches the energy target (~300 Wh/dm^3) and for few battery technologies, it can provide the needed power (~2 kW/kg). For this reason, SC and LIC have been excluded from our trade-off and research has been focused on sizing an optimized pack of batteries. In addition, having over energy in the pack (typically 200 Wh/dm^3 vs 60 Wh/dm^3 as target) is very beneficial to improve LIB performances. As a matter of fact, the battery that has a State Of Charge (SOC) from 30 to 70% all time will have certainly a more extended lifetime than the one working from 10 to 90%.

Some comments are important about datasheets on LIB densities.

- Sometimes, the power density is given for maximum current in a short time (e.g. 1 s or 10 s). That's why we may find in datasheets higher densities than the ones in this paper. However, these values are not useful except for a short duration which is not our case.
- In some cases, the maximum current or the C-rate is higher in discharge than in charge. The power density is given with respect to the highest possible current to be delivered, what is not totally accurate. For example, the Kokam's products have typically a discharge C-rate around 20 whereas only 1C in

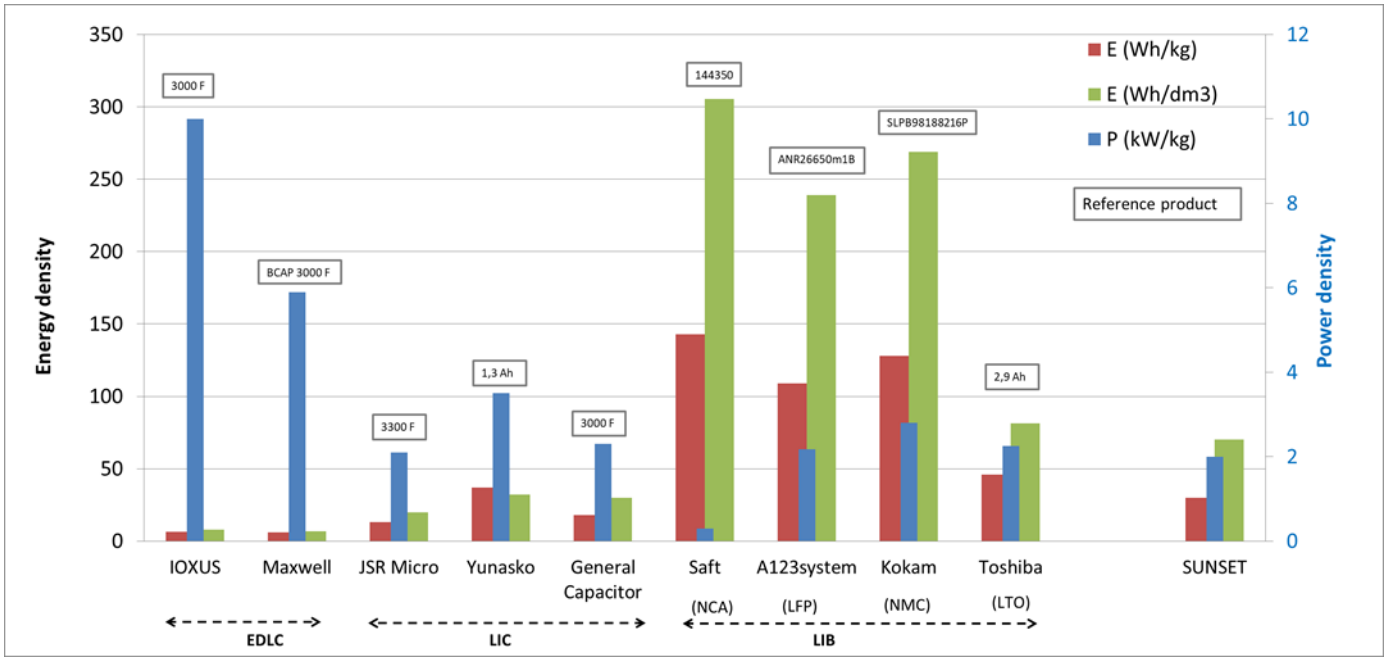

Fig.3 Power and energy densities according to the market suppliers.

charging (SLPB 8043128H [9]).

For this issue, Kokam product will not be studied in our preliminary design in the next subsection. However, this kind of technology would be very beneficial for very slow charge but very fast discharge applications.

- Working at the highest current is feasible from the cell standpoint. But one should verify if taking into account the losses due to the Equivalent Series Resistance (ESR), the efficiency of the pack batteries is still worthy. Therefore, the effective ESR in the cell is not the one that is usually given in the datasheet at 1 kHz. This latter represents only one point (at 1 ms) of the characteristic curve. To calculate the actual power losses, the ESR should be measured during several seconds instead of 1 ms.

As a result, designers have to be careful about announced values in datasheets and figure out in what conditions the tests have been performed (temperature, duration, SOC, rest…).

C. *Preliminary design*

The following study presents the A123system and Toshiba solutions. ESS will be designed assuming an average power of 50 kW and 700 Wh to compare the two solutions on a same basis.

1) A123system ANR26650 LFP cell

The main cell characteristics are: (3.3 V; 2.5 Ah) and (72 g; 0.0344 dm^3). The ESR has been extrapolated from the datasheet at 35°C at different SOC [10] (see Fig. 4). The Fig. 5 shows the picture of A123system cell at the left and the simple model that helps to deduce the equations (1) and (2). Then the maximum allowable current (I_{max_charge} and $I_{max\_discharge}$) has been calculated and presented in Fig. 6 in order to protect the cell from undervoltage (< 1.8 V) and overvoltage (> 3.8 V) using both equations. From Fig. 6, we observe that this cell is asymmetric; i.e. the maximum current in discharge is very high compared to charge current. Once the datasheets deal with our application conditions, the sizing would be done straightforwardly. First, the preliminary sizing is done according to fixed values (nominal voltage and current) regardless the SOC. Second, several iterations should be done to re-verify power capacity and current limit taking into account ESR and Open Circuit Voltage (OCV) at different SOC.

$$U_{overvoltage} = OCV + I_{max\_charge}\ ESR \quad (1)$$

$$U_{undervoltage} = OCV - I_{max\_discharge}\ ESR \quad (2)$$

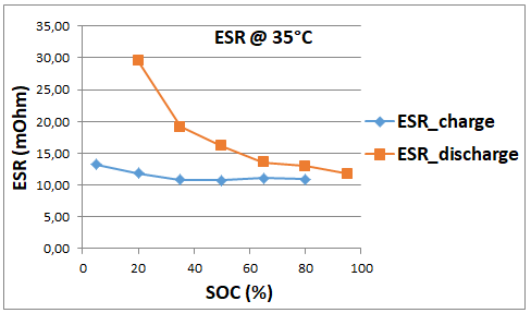

Fig. 4. Extrapolated ESR of ANR26650 at 35°C.

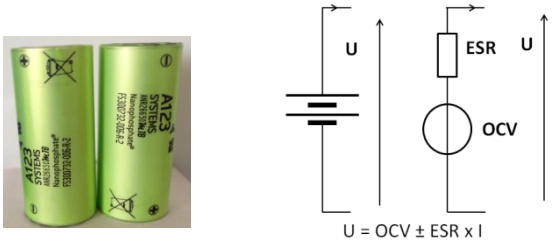

Fig. 5. A123system cells (right) and the typical model (left).

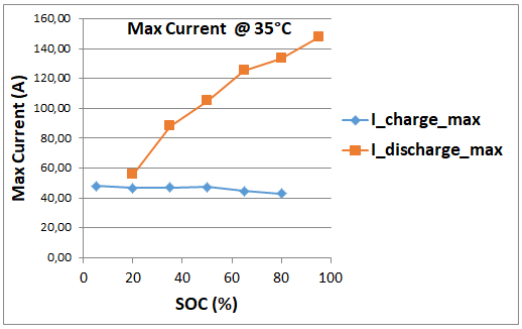

Fig. 6. Calculated current for 30 seconds of ANR26650 at 35°C.

Assuming that maximum allowable current in charge/discharge at 35°C is 50 A for 30 seconds, the following sizing could take place:

- U = P/I= 50000/50 = 1000 V. Considering three branches of 333 V each, we will have:
- Number of cells N = 333/3,3 = 101 => 3p101s (i.e. 3 branches in parallel of 101 cells in series)
- Weight = 0.072*101*3 = 21.8 kg
- Volume = 0.0344*101*3 = 10.45 dm^3
- Embedded Energy = I(Ah)*U_cell (V)*N = 2.5*3.3*101*3 = 2500 Wh

At this stage, it is important to calculate the evolution of the voltage per branches which depends on SOC and the current involved. At each SOC (from 5 to 95%) we have calculated the voltage using the maximum allowable current without exceeding the nominal power (50 kW). The orange curve in Fig. 7 illustrates how the voltage drops from 340 V to 270 V during discharging due to the ESR. The signs indicate that the voltage decreases while SOC decreases (and OCV as well) from 95% to 5%. In contrary the blue curve shows the positive drop voltage from 320 V to 380 V when the cells are charged from 5% to 95%. This curve is essential for the next section while designing the power converter.

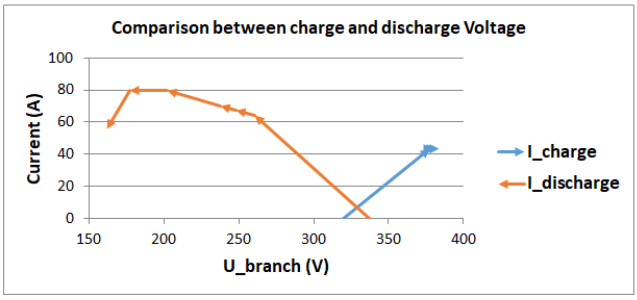

Fig. 7. A123system solution: voltage evolution across branch regarding charge and discharge current.

The power losses depend on the ESR and the current involved. As said, ESR highly depends on SOC and temperature. At this stage we will calculate the maximum losses (Fig. 8) in function of SOC based on the maximum current (Fig. 7) at only the operation temperature (35°C). The ESR and current discharge are higher in discharge which explains the higher discharge losses.

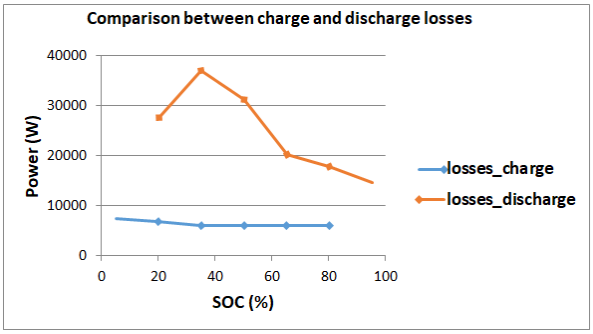

Fig. 8. A123system solution: comparison of charge and discharge power losses in function of SOC.

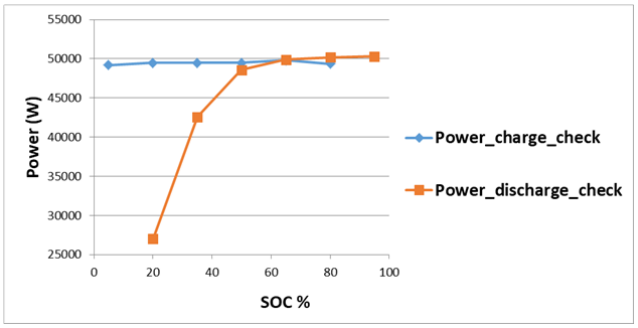

Fig. 9. A123system solution: discharge and charge power capability taking into account maximum current in two cases.

Finally, from Fig. 9, the power that could be recovered is 50 kW at all SOC values whereas it is limited for generation at 27 kW at 20% of SOC. This latter limitation is basically due to the current limitation and high losses at low SOC.

2) Toshiba LTO cell

According to the Toshiba datasheet [11], the 2.9 Ah cell (2.4 V;150 g; 0.0855 dm^3) may reach 80% of SOC in one minute (0.016 hour). Besides, the necessary time to charge a battery is evaluated as:

$$T\,(h) = Q\,(Ah) / I\,(A) \qquad (3)$$

Given the duration and the percentage of plain capacity, the current can be deduced as follows
I(A) = 2.9*0.8/0.016= 145 A.

The maximum current may then reach 145 A per cell for a short time (less than 60 seconds). The following sizing has been based on the current of 140 A.

- U=P/I=50kW/140A= 358 V
- Number of cells N= 358V/2.4V= 148 => 1p148s (one branch of 148 cells in series)
- Weight = 0.15*148= 22.2 kg
- Volume= 0.0855*148= 12.66 dm^3
- Embedded Energy = 2.9*2.4*148= 1030 Wh

The same approach has been used to pre-design the storage pack using Toshiba cells. Notice that ESR is almost constant in charge and discharge and also for all SOC values (3.5 mΩ at 30 seconds pulse). The current falls down at high voltage to avoid overvoltage cell (Fig. 10). The maximum power losses are presented in Fig. 11. As it can be seen from Fig. 12, the maximum power charge (50 kW) is reached out even with a current lower than 140 A. However, the capability of charging at high SOC decreases until 34 kW. Thus, the power that could be recovered is between 34 kW and 50 kW depending on the SOC value.

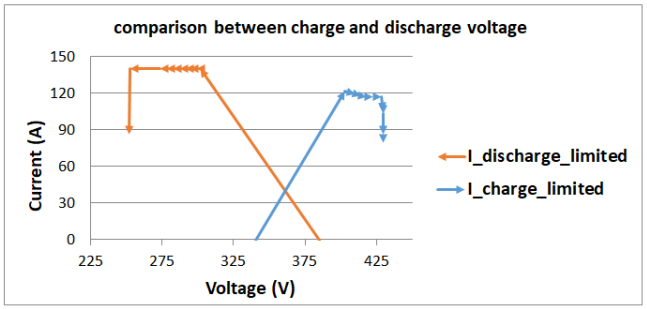

Fig. 10. Toshiba solution: voltage evolution across branch regarding charge and discharge current.

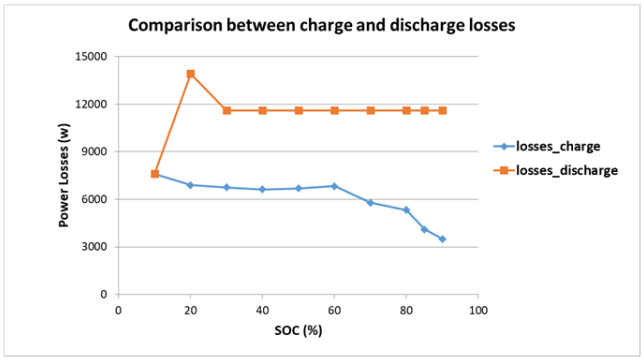

Fig. 11. Toshiba solution: comparison of charge and discharge power losses in function of SOC.

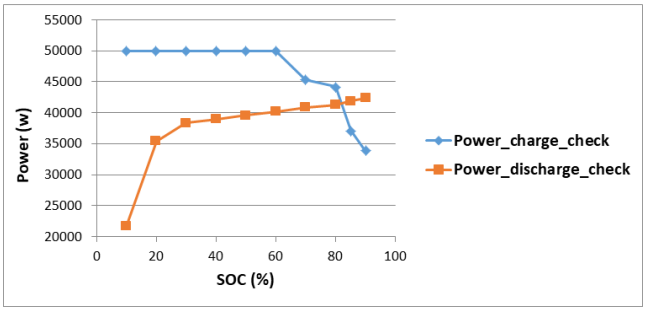

Fig. 12. Toshiba solution: discharge and charge power capability taking into account maximum current in two cases.

3) Discussion

The table I summarizes the results of the pre-design of the storage system using the A123system 2.5 Ah and Toshiba 2.9 Ah cells. As it can be seen, both solutions are feasible and meet the densities target. Obviously, the LTO technology shows a better trade-off because the efficiency is higher which reduces enormously the heater sink. Both solutions have exceeded the energy target as expected even if

the ratio is bigger in LFP. According to the literature LTO has better life cycle than LFP. But this latter statement could not be generalized because it depends on Depth of Discharge of the battery. Under our assumption of energy, the 700 Wh constitute 67 % DoD of Toshiba cells but only accounts for 28 % of A123system cells.

TABLE I. Comparison of the battery pack using A123system and Toshiba cells

	A123system 2.5 Ah ANR26650 (LFP)	Toshiba 2.9 Ah SCiB (LTO)
Max current (A)	80	140
Voltage /branch (V)	140 – 380	250 – 430
Volume (dm^3)	10,45	12,66
Weight (kg)	21,816	22,20
Embedded Energy (Wh)	2500	1030
Power charge (kW)	50	50
Power density (kW/kg)	2.3	2.25
Energy density (Wh/dm^3)	239	81.7
Efficiency (%)	50 – 85	77 - 90
Safety	++	+
Application compliance level	+	++

However, according to our calculation, the LTO are unable to keep charging 50 kW at high SOC which is equivalent to say: at high SOC we can't recover the total energy from the braking which is the main goal of this SUNSET module. On the other hand, LFP has more stability than LTO which represents a higher safety level [12]. All these parameters should be taken into account but also environment conditions such as certification. Unfortunately, due to the lack of qualification in aeronautic domain, the Toshiba technology may be discarded.

III. Power Converter

Power converters in hard-switching operation, larger than 10 kW are often based on Silicon IGBTs (Insulated Gate Bipolar Transistor) [13]. The operating frequency is mostly limited by switching losses to around 20 kHz, hence this has an impact on the size and mass of capacitors and inductors. One of the main objectives of SUNSET pre-design is to detect the most suitable recent power converter architecture compatible with a nominal power up to 50kW [14].

A. Trade-off

The aircraft HVDC network is a balanced symmetrical bus between +270V and -270V (typically 540V). The midpoint will be used in order to reduce the voltage constraints on the transistors and the inductances. Therefore, it reduces the volume and losses in these latter components. As seen in the previous section, the necessary voltage to reach power and energy targets for both solutions is between 140-430 V. The ratio between bus voltage and the latter level can be converted without requiring a transformer. Moreover, as seen in Fig. 13, the converter should be bidirectional: recovering energy while braking when operating as a buck, then discharging batteries to the HVDC when operating as a boost. Moreover, a galvanic isolation is not necessary because the battery pack offers a floating voltage source.

Battery charging from recovery and discharging into a DC-bus requires a power switch capable of bidirectional current flow, bidirectional voltage blocking for proper power management. In such a case, the bidirectional power switch (BPS) is unavoidable. The latter should be able to block voltage in OFF-state to avoid draining a charged battery or to avoid one battery from charging into another battery in case of several branches in parallel. The BPS should be able to support inrush current as well as helps reducing it with high-frequency operation.

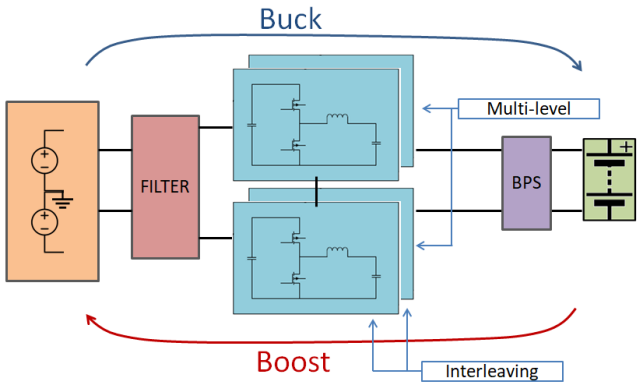

Fig. 13. Architecture synoptic of the SUNSET.

B. Preliminary design

The design of the converter will dependent on many parameters of which:

- Frequency: the desire for smaller size calls for increasing the switching frequency. But increasing the operating frequency causes more switching losses in active devices what reduces the efficiency of the power module. A trade-off should be set to reduce both volume and losses. In our application, a study has shown that a suitable switching frequency is above 100 kHz.
- Multilevel order: in all cases, two levels should be used to reduce the voltage constraints.
- Interleaving: basically, each branch in the battery pack involves a converter in order to isolate any current draining or defaults. For example, A123system solution needs three converters of 16.6 kW for each branch whereas Toshiba solution needs only one 50 kW converter. The number of legs (half-bridge) per converter relies on the nominal current value [15]. Our study has shown that two interleaved phases are necessary for the A123system solution (50 A) and three phases for Toshiba solution (140 A). In the latter solution two transistors should be put in parallel for each switch.

  Fig. 14 shows an example of two-level and two interleaved phase converter. Three converters (16.6 kW) of this topology will be necessary for the A123system solution.

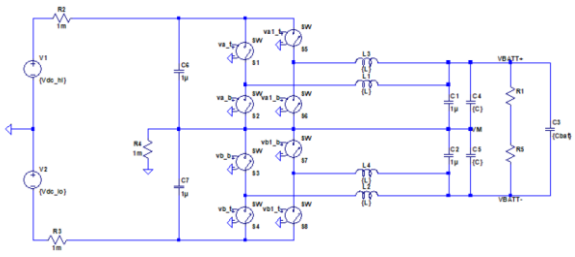

Fig. 14. Two-level and two interleaved phases as a bidirectionnal converter.

Considering the maximum battery pack voltage (490V) and taking into account the voltage derating to ensure reliability, transistors must have a breakdown voltage larger than 600V. In addition, their nominal current must be larger than 50 A. So the operating transistor conditions would be at least (650 V, 75 A).

It worth noting that design of a BPS is a very crucial step:

- Since branches are in parallel and do not have exactly the same potential, one branch may charge into another one. To avoid this process, as seen in Fig. 15, the number of BPS should be equal to the number of branches.
- The BPS should provide low on-state resistance (R_{DSon}) for tight voltage regulation during charging phase and for better battery capacity utilization in back-up mode.
- The BPS device is always connected to the battery side so it should draw very low leakage current.
- An example of a BPS configuration is given in Fig. 15-b. The transient voltage and current should be studied appropriately to choose the MOSFETs that may support these constraints.

As a consequence, the high current value involved in the Toshiba solution imposes a larger silicon size of MOSFET than in the A123system solution. However, in the latter case, three BPS should be implemented.

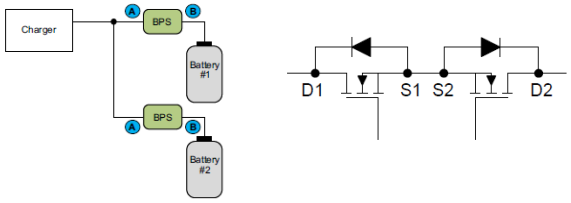

Fig. 15. BPS in a Power System like SUNSET: (a) schematic of a 2-branch configuration (b) configuration of a BPS: Back-to-Back N-MOSFETs in common-Source.

Finally, Table II shows the comparison of main converter specifications between the two solutions. The weight and volume of the electronic components (especially semiconductors and inductances) are in favour of the Toshiba solution.

TABLE II. Comparison of converter main specifications for A123system and Toshiba cells

Converter	A123system	Toshiba
Number of converter	3	1
Number of legs	2	3
Level	2	2
BPS	3	1
Weight	+	++
Volume	+	++
Losses	+	++

IV. Conclusion

This paper has shown a global study to pre-design a specific module dedicated to the Electric Taxiing. This function is an important step towards the more electrical aircraft. The trade-off has shown a feasible preliminary design of a battery pack with sufficient energy density (higher than 60 Wh/dm^3) but with modest power density (2.2 kW/kg). The main limitation is the high ESR of cells in comparison to LIC and thus the lower efficiency. A two-level and two interleaved phase converter appears as a good candidate to associate with the battery pack. A complete prototype is expected to be manufactured in the next months.

Acknowledgment

This project has received funding from the Clean Sky 2 Joint Undertaking under the European Union's Horizon 2020 research and innovation programme under grant agreement n°785585.*

*This output reflects only the author's view and that the JU is not responsible for any use that may be made of the information it contains.

References

[1] R. Tom, "Air Transport Statistics, Extract from Aviation and The Environment published by the Parliamentary Office for Science and Technology (UK)," 2011.

[2] M. Farhadi, S. Member, and O. Mohammed, "Energy Storage Technologies for High-Power Applications," *IEEE Trans. Ind. Appl.*, vol. 52, no. 3, pp. 1953–1961, 2016.

[3] "Fuel Consumption and Emissions from Airport Taxi Operations," *Environ. Lead. (6/29/09), quoted from a Rep. by EADS Airbus*.

[4] P.-H. Huang, J.-K. Kuo, and C.-Y. Huang, *A new application of the UltraBattery to hybrid fuel cell vehicles*, vol. 40. 2015.

[5] S. Chauque, F. Y. Oliva, A. Visintin, D. Barraco, E. P. M. Leiva, and O. R. Cámara, "Lithium titanate as anode material for lithium ion batteries: Synthesis, post-treatment and its electrochemical response," *J. Electroanal. Chem.*, vol. 799, no. May, pp. 142–155, 2017.

[6] M. A. Hannan and S. Member, "State-of-the-Art and Energy Management System of Lithium-Ion Batteries in Electric Vehicle Applications : Issues and Recommendations," *IEEE Access*, vol. 6, pp. 19362–19378, 2018.

[7] A. Burke, "Ultracapacitor technologies and application in hybrid and electric vehicles," *Int. J. energy Res.*, vol. 31, no. August 2007, pp. 135–147, 2007.

[8] N. E. Ghossein, A. Sari, and P. Venet, "Nonlinear Capacitance Evolution of Lithium-Ion Capacitors Based on Frequency- and Time-Domain Measurements," *IEEE Trans. Power Electron.*, vol. 33, no. 7, pp. 5909–5916, 2018.

[9] "Kokam company." [Online]. Available: http://kokam.com/cell/. [Accessed: 20-Nov-2018].

[10] "A123system." [Online]. Available: http://a123batteries.com/. [Accessed: 20-Jan-2019].

[11] "Toshiba." [Online]. Available: https://www.scib.jp/en. [Accessed: 02-Feb-2019].

[12] T. Horiba, "Lithium-Ion Battery Systems," *Proc. IEEE*, vol. 102, pp. 939–950, 2014.

[13] M. Vellvehi and P. Devices, "Analysis of Bidirectional Switch Solutions Based on Different Power Devices," 2017.

[14] A. A. Khan, H. Cha, and H. Kim, "A Family of High Efficiency Bidirectional DC-DC Converters Using Switching Cell Structure," *2016 IEEE 8th Int. Power Electron. Motion Control Conf. (IPEMC-ECCE Asia)*, pp. 1177–1183, 2016.

[15] Y. Zhang, Y. Gao, J. Li, and M. Sumner, "Interleaved Switched-Capacitor Bidirectional DC-DC Converter With Wide Voltage-Gain Range for Energy," *IEEE Trans. Power Electron.*, vol. 33, no. 5, pp. 3852–3869, 2018.